Tellus (2005), 57A, 662–675
Printed in Singapore. All rights reserved

TELLUS

Why ocean heat transport warms the global mean climate

By CELINE HERWEIJER[1]*, RICHARD SEAGER[1], MICHAEL WINTON[2] and AMY CLEMENT[3], [1]*Lamont Doherty Earth Observatory of Columbia University, New York, USA;* [2]*Geophysical Fluid Dynamics Laboratory/NOAA, Princeton, USA;* [3]*Rosenstiel School of Marine and Atmospheric Sciences, University of Miami, USA*

(Manuscript received 20 April 2004; in final form 22 November 2004)

ABSTRACT

Observational and modelling evidence suggest that poleward ocean heat transport (OHT) can vary in response to both natural climate variability and greenhouse warming. Recent modelling studies have shown that increased OHT warms both the tropical and global mean climates. Using two different coupled climate models with mixed-layer oceans, with and without OHT, along with a coupled model with a fixed-current ocean component in which the currents are uniformly reduced and increased by 50%, an attempt is made to explain why this may happen.

OHT warms the global mean climate by 1 to 1.6 K in the atmospheric general circulation (AGCM) ML model and 3.5 K in the AGCM fixed current model. In each model the warming is attributed to an increase in atmospheric greenhouse trapping, primarily clear-sky greenhouse trapping, and a reduction in albedo. This occurs as OHT moistens the atmosphere, particularly at subtropical latitudes. This is not purely a thermodynamic response to the reduction in planetary albedo at these latitudes. It is a change in atmospheric circulation that both redistributes the water vapour and allows for a global atmospheric moistening—a positive 'dynamical' water vapour feedback. With increasing OHT the atmospheric water vapour content increases as atmospheric convection spreads out of the deep tropics. The global mean planetary albedo is decreased with increased OHT. This change is explained by a decrease in subtropical and mid-latitude low cloudiness, along with a reduction in high-latitude surface albedo due to decreased sea ice. The climate models with the mixed layer oceans underestimate both the subtropical low cloud cover and the high-latitude sea ice/surface albedo, and consequently have a smaller warming response to OHT.

1. Introduction

The oceans react to the radiation surplus at low latitudes and the deficit at high latitudes by moving heat from the equatorial regions to the poles, cooling the former and warming the latter. One might think that this heat transport simply redistributes heat, leaving the global mean surface temperature unaltered. However, if the climate adjusts to changes in ocean heat transport (OHT) by way of a change in the distribution and effectiveness of its radiative absorbers and reflectors—clouds, water vapour, sea ice and land snow—a shift in the global mean surface temperature could ensue.

By most accounts, movement of heat by the oceans causes the global mean climate to be warmer than it otherwise would be. Most well known, perhaps, is the capacity of OHT to constrain the extent of winter sea ice and thus reduce the planetary albedo (Rind and Chandler, 1991; Poulsen et al., 2001; Lewis et al., 2003; Winton, 2003). Nonetheless, in the present climate the importance of the sea ice–albedo feedback is restricted to small regions of the high-latitude oceans where, anyway, OHT is overwhelmed by atmospheric heat transport (AHT). In contrast, equatorward of 17°, the ocean moves more heat polewards than the atmosphere (Trenberth and Caron, 2001). Recent studies using coupled atmosphere–ocean box models (Clement and Seager, 1999) and atmospheric general circulation models (AGCMs) coupled to simplified oceans (Gregory and Mitchell, 1997; Clement and Seager, 1999; Winton, 2003) have suggested that tropical OHT causes a reduction in subtropical low cloudiness, decreases planetary albedo and, once again, causes a global mean warming. In contrast, in the context of AGCMs, less attention has been given to understanding the potential influence of OHT on the water vapour feedback mechanism. How OHT affects the global mean temperature through its impact on the distribution and possibly the total amount of atmospheric moisture, and thus atmospheric greenhouse trapping, remains poorly understood. All of the above climatic adjustments to OHT will

*Corresponding author.
e-mail: celineh@ldeo.columbia.edu
LDEO Contribution No. 6701

be investigated here. It will be shown that due to a change in atmospheric circulation the primary reason for warming by OHT is, in fact, an increase in global mean greenhouse trapping.

Understanding the impact of OHT on the mean global climate is not only of considerable interest to the study of basic climate dynamics but may have some relevance to understanding past and future climate change. Should the relative partitioning between OHT and AHT change, the planet's regional and global mean climates could also be affected. The warmer climates of the Mesozoic and Tertiary may have seen estimated global OHT increases of 15–70% according to palaeoclimate model simulations with modern day CO_2 values (Rind and Chandler, 1991). With respect to future climate change, purely hypothetically, were greenhouse warming to lead to increased partitioning of poleward heat transport towards the atmosphere a negative climate feedback would occur. Furthermore, as a change in OHT affects the global energy balance, it will act as a positive feedback for other types of forcing (such as altered CO_2 and variations in insolation), thus potentially playing a role in scenarios of rapid climate change.

Held (2001) considered heat transport (HT) by coupled meridional overturning circulations and argued that poleward atmosphere and ocean heat transport in the tropics is constrained by the static stabilities of each fluid, making it difficult to change their relative partitioning. However, Hazeleger et al. (2004) show that once transport by the equatorial gyres is considered, tropical OHT can vary in a way that may confound this simple reasoning. Stone (1978) argues that the fundamental constraint is that the total poleward heat transport remains fixed, such that changes in AHT and OHT compensate each other, a case also made by Bjerknes (1964) and demonstrated by a number of modelling studies (Manabe et al., 1975; Clement and Seager, 1999; Cohen-Solal and Le Treut, 1997). While the dynamics by which such a compensation could occur remain to be worked out, a possibly varying OHT highlights the need to understand the effect of OHT on climate. Recent evidence alone, showing a slowdown of the shallow meridional overturning circulation (MOC) and thus reduced OHT in the tropical Pacific since the 1970s, consistent with the observed surface ocean warming (McPhaden and Zhang, 2002), highlights that this is not purely an academic matter. Trying to understand how OHT affects the distribution and number of radiative absorbers and reflectors could instead offer important insights into the mechanisms of climate change and variability on long timescales.

Here we shall investigate the means by which OHT warms climate using AGCMs coupled to two kinds of simplified ocean. The first employs the '*q*-flux' approach of Clement and Seager (1999), hereafter referred to as C&S, in which a conventional mixed-layer ocean, with and without OHT, is coupled to two different AGCMs. The second involves a kinematic ocean, following the fixed current approach described in Winton (2003) in which fixed fields of ocean currents that advect heat and salt are uniformly decreased and increased by 50%. A multimodel approach is chosen as it is acknowledged that the responses of water vapour, cloud and radiation to altered OHT are also dependent on the convective and cloud parametrizations in the models. All three coupled model experiments will be compared in order to identify the features that are robust and to examine the range of those that are more model or approach specific. We will attempt to explain why OHT warms the global mean climate.

Two important points must be addressed regarding the artificiality of the model experiments. First, in the real world, the oceanic and atmospheric circulations are part of a coupled system and not specified independently as in our model simulations. For example, the surface trade winds are essential in driving the ocean heat flux by both the meridional overturning cells and the ocean gyres. An altered OHT would give rise to altered atmospheric circulations which would then feed back on the heat transport by the wind-driven ocean circulation. Second, the experiments we perform are highly theoretical in that they involve an unrealistically large 100% change in OHT. With the aforementioned caveats in mind, the artificiality of the model experiments does have an advantage in that it enables us to isolate key components of the climate system and examine them in a controlled context.

We will suggest that a primary reason for warming by OHT is that the atmosphere moistens, particularly at subtropical latitudes, and traps more terrestrial radiation. The reduction in planetary albedo related to a decrease in sea ice/land snow and low cloudiness also plays an important role. These results are found in all three coupled-model experiments studied. The global warming response to increased OHT must be accomplished by the change in atmospheric circulation, driving changes in the distribution of clouds and atmospheric water vapour. The subsequent section presents details of the models and experimental designs. The third section presents the mechanisms whereby OHT warms the climate via its effect on sea ice and land snow, clouds, water vapour and the atmospheric lapse rate. The discussion and conclusions will be presented in Section 4.

2. Models and experimental design

2.1. q-flux experiments: OHT versus no OHT

Here we employ the simplest type of sensitivity study: one in which the atmosphere is coupled to an ocean mixed layer (OML) in which the heat transport is accounted for, and one in which the effect of OHT is removed (C&S). In order to assess the reproducibility of the results obtained, these experiments will be carried out with two different AGCMs coupled to two different OMLs.

As in C&S, we evaluate experiments using the nine-vertical-layer 4° by 5° resolution Goddard Institute for Space Studies (GISS) model version II (Hansen et al., 1983). This model includes prognostic clouds and liquid water vapour, up-to-date radiation and convection parametrizations, realistic land–sea

distribution and orography, and a thermodynamic sea ice model (Del Genio et al., 1996). The OML has two vertical layers, with variable mixed-layer depth specified from observations. The 'control' experiment was run for 20 yr. It consists of an AGCM coupled to an OML with a specified OHT. This q-flux has been diagnosed as that required for the model to reproduce the observed SST (Russell et al., 1985). The sea ice cover is computed in this model. In a second experiment, the q-flux was set to zero everywhere (i.e. the 'no flux' case) and run over an equivalent time interval. The same approach was used with a slab 75 m deep OML coupled to the National Center for Atmospheric Research Community Climate Model (CCM3; Kiehl et al., 1998), run with T42 resolution and 18 vertical layers. This model has fixed ice cover.

The model and satellite-derived fluxes of net surface short-wave radiation (SWR) were compared to assess the radiative impact of the underestimation of boundary layer cloud cover over the eastern tropical oceans in the models (Seager et al., 2003). Surface SWR data from the Earth Radiation Budget Experiment (ERBE; Li and Leighton, 1993) and the International Satellite Cloud Climatology Project (ISCCP; Bishop and Rossow, 1991) were used, noting that the derived ISCCP flux is higher than the derived ERBE flux at all times and locations (Seager and Blumenthal, 1994). No consistent overestimation of the surface short-wave (SW) flux over the eastern tropical oceans was found in either model. On a zonal mean, the annual net SWR in the control GISS and CCM3 coupled models appears to capture the observed values reasonably well. Both models slightly overestimate the tropical SWR in relation to the ERBE data set (particularly CCM3 by 20 W m^{-2}) while underestimating this flux by a similar amount with respect to the ISCCP data. The 'q-flux' term will thus be considered to generally be a reasonable representation of the OHT, particularly in the zonal mean.

2.2. *Fixed current experiments: 150% versus 50% current strength*

An alternative approach, described in detail by Winton (2003), uses fixed fields of ocean currents to advect heat and salt in a 3-D ocean model. The currents for the ocean model come from a Geophysical Fluid Dynamics Laboratory (GFDL) climate model simulation. To explore the role of OHT, these currents are uniformly reduced and increased by 50%. Winton (2003) has shown that the heat transport changes roughly in proportion to the current weakening/strengthening. Variability associated with ocean dynamical responses is eliminated. It is important to note that to some extent we may be observing climate transients as this approach incorporates the full depth of the ocean. In particular, the global mean SST has not quite reached steady state at the end of the integrations (see Winton, 2003, Fig. 4).

The atmosphere/land component used in the fixed current coupled experiments is the developmental version of the GFDL AM2 model (The GFDL Global Atmospheric Model Development Team, 2004). The model (hereafter referred to as GFDL) has 2.5° latitude by 2.0° longitude resolution and 18 levels in the vertical. This model includes radiative treatment of H_2O, O_3, CO_2, N_2O, CH_4, and four CFCs, a modified relaxed Arakawa–Schubert (RAS) mass flux scheme for moist convection, a large-scale cloud scheme with liquid, ice and cloud fraction as prognostic tracers, a Mellor–Yamada 2.5 turbulence closure vertical mixing scheme, and a land component with five layers for temperature (Winton, 2003). GFDL's IM2 elastic-viscous plastic sea ice model is used in the experiments (see Winton, 2003, for a description). The experiments were run for 100 yr with climatologies constructed from the last 20 yr of the integrations.

3. Results

OHT has a substantial impact on the distribution of sea ice, clouds, atmospheric water vapour and consequently on the top of the atmosphere (TOA) radiative fluxes. Introducing or increasing OHT in all three coupled models results in a global mean warming ranging from 1–1.6 K in the q-flux experiments, to 3.5 K in the 150% strength minus the 50% strength fixed current experiment. This requires either an increase in the greenhouse trapping and/or a decrease in planetary albedo. However, if the models have reached equilibrium the annual mean net radiation at the TOA must be unchanged. This is essentially so when OHT is introduced into the mixed-layer coupled models (Table 1) and is

Table 1. Global mean changes due to OHT in all three coupled model experiments

Δvariable	GISS (control—no flux)	CCM3 (control—no flux)	GFDL (150%–50% currents)
Δsurface temperature	1.0 K	1.6 K	3.5 K
ΔSST	1.1 K	0.9 K	2.4 K
Δtotal OLR	0.7 W m^{-2}	2.1 W m^{-2}	5.0 W m^{-2}
Δtotal SW at TOA	0.8 W m^{-2}	2.2 W m^{-2}	5.6 W m^{-2}
Δtotal G_t	3.3 W m^{-2}	6.5 W m^{-2}	11.9 W m^{-2}
ΔSW reflected at TOA	−0.8 W m^{-2}	−2.9 W m^{-2}	−5.6 W m^{-2}
ΔM_q	–	1.62 kg m^{-2}	4.05 kg m^{-2}
Δlow clouds	0.5%	−2.0%	−4.4%
Δmid-clouds	−0.9%	−1.9%	−1.3%
Δhigh clouds	1.2%	0.5%	−0.5%

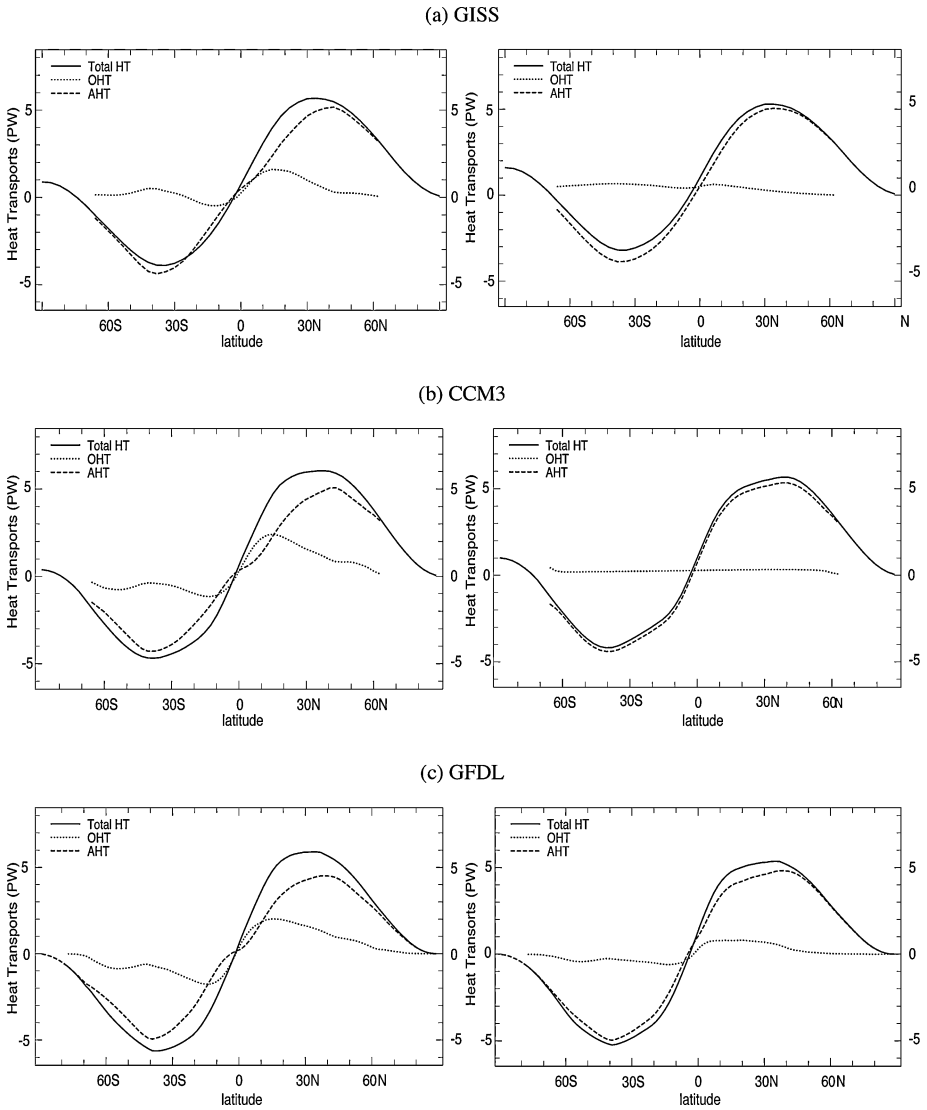

Fig. 1. Northward annual mean heat transport in the atmosphere plus ocean (Total HT), atmosphere only (AHT) and ocean only (OHT) (where applicable) for (a) GISS AGCM OML control (left) and no OHT (right), (b) CCM3 AGCM OML control (left) and no OHT (right) and (c) GFDL AM2 AGCM dynamic ocean 150% fixed current strength (left) and 50% fixed current strength (right). Units of heat transport presented are PW (10^{15} W).

almost the case using the kinematic ocean of the fixed current experiments. However, the degree of transience associated with timescales of the full ocean depth in the fixed current experiments permits a small radiative imbalance at the TOA.

First we address the extent of compensation between the atmosphere and ocean heat transport outlined in the Introduction. Figure 1 shows the annual mean meridional heat transport and the relative partitioning of this flux between the atmosphere and ocean for each of the model experiments. The net transport is that required by the energy balance at the TOA, with the atmospheric transport obtained by subtracting the OHT from the total transport. The OHT itself is derived from the annual mean net surface heat flux. In the experiments in which the q-flux is set to zero (the no OHT case), some apparent, but very small, OHT remains indicating that equilibrium has not been fully reached (Figs 1a and b). It can be seen that in all three coupled models the AHT adjusts to compensate for the change in OHT in agreement with other GCM experiments (e.g. Manabe et al., 1975; Cohen-Solal and Le Treut, 1997; Clement and Seager, 1999). In the deep tropics, where the OHT is largest, the compensation is almost complete. Elsewhere, the total HT is slightly greater when the OHT is included or increased. In each model the total HT out of the tropics, i.e. the sum of that across 30° N and 30° S, is increased by approximately 1 PW when OHT is increased. Consequently at these latitudes the atmosphere compensates for only half of the change in OHT. Because of this, when OHT

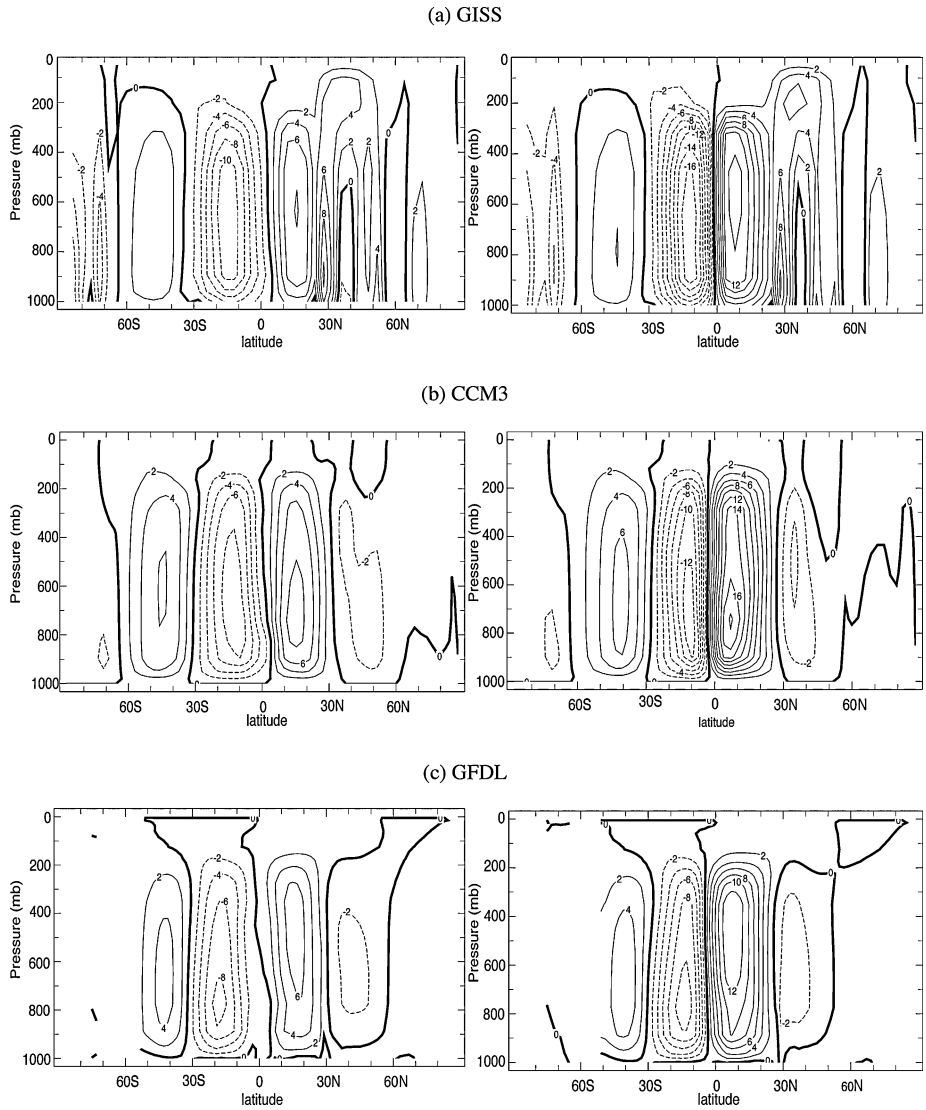

Fig. 2. The annual mean difference in the atmospheric meridionally overturning stream function, Ψ in 10^{10} kg s^{-1}, for (a) GISS AGCM OML control (left) and no OHT (right), (b) CCM3 AGCM OML control (left) and no OHT (right) and (c) GFDL AM2 AGCM dynamic ocean 150% fixed current strength (left) and 50% fixed current strength (right).

is included or increased, the net radiative gain in the tropics is increased. As we shall see this is accomplished by an increase in greenhouse trapping in the tropics and a reduction in the low cloud cover and albedo.

Figure 2 shows the atmospheric meridional overturning stream function in each of the model experiments. The largest change in the meridional overturning circulation occurs at low latitudes where OHT dominates the total heat transport. Here the reduction of AHT that occurs when OHT is included, or increased, is accomplished by a halving of the strength of the Hadley cell (Fig. 2). In the *q*-flux experiments the compensation of tropical AHT for the change in OHT means the tropical mean (30° N to 30° S) TOA balance changes by very little. It is noted that the feedback of the associated surface wind-stress change on the ocean circulation that would occur in a fully coupled system is not captured in these experiments.

3.1. Mechanisms whereby OHT warms the mean global climate

Although the AHT largely compensates for changes in the OHT this does not mean the global mean temperature will remain the same. The atmospheric adjustment to changes in OHT may involve changes in albedo and greenhouse trapping that require a change in the global mean temperature.

Figure 3 shows the change in zonally averaged SWR reflected at the TOA and the atmospheric greenhouse trapping associated with introducing or increasing OHT in the coupled model

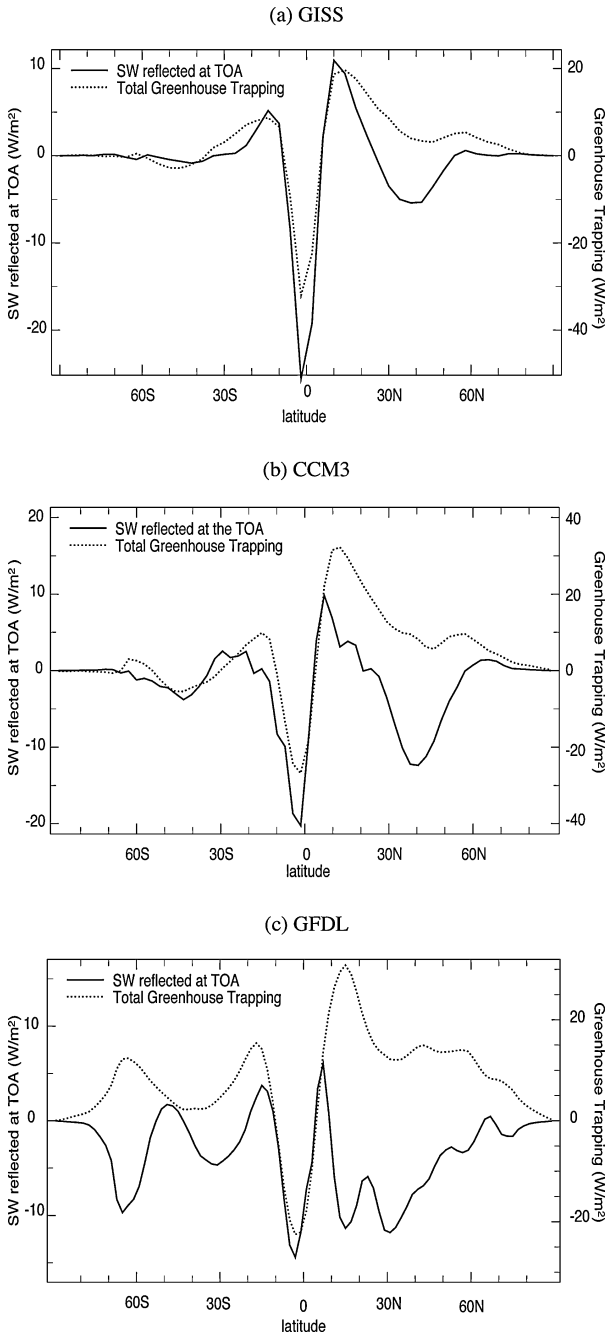

Fig. 3. The annual mean difference in the zonally averaged, area-weighted SWR reflected at the TOA and total greenhouse trapping due to OHT (both in W m^{-2}): (a) control—no flux, GISS AGCM OML, (b) control—no flux, CCM3 AGCM OML, (c) 150%–50% fixed currents, GFDL AM2 AGCM dynamic ocean.

experiments. Here greenhouse trapping, G_t, represents the amount of long-wave radiation emitted (OLR, outgoing long-wave radiation) from the surface that does not escape into space due to absorption by water vapour in the atmosphere ($G_t = \varepsilon\sigma T_s^4 - \text{OLR}$). In all three models the net TOA radiation in the deep tropics (10° S–6° N) remains approximately unchanged when the oceans transport more heat. More striking is the substantial increase in greenhouse trapping in the surrounding tropics and subtropics. In this same region, most notably in the GFDL model, the planetary albedo reduces under strengthened OHT (Fig. 3c). If, as is the case, the net TOA radiation balance is restored in equilibrium, both the increase in G_t and the albedo reduction require a climate warming. The GFDL model is also the only model to show a significant high-latitude response when the OHT is increased.

In the global mean, the change in reflected SWR at the TOA and atmospheric greenhouse trapping is such that OHT warms the global mean climate—with the increase in greenhouse trapping dominating the response (Table 1). Understanding the mechanisms behind this global response to OHT requires reference to the latitudinal signature of the radiative changes shown in Fig. 3. Fundamentally, any change in the radiative fluxes at the TOA must be explained in terms of changes in surface albedo, cloud albedo and atmospheric opacity due to clouds, water vapour and the atmospheric lapse rate. We will now outline these changes.

3.1.1. The role of sea ice and land snow. The primary effect of altered OHT on high-latitude climate concerns its impact on the distribution of sea ice and land snow. The resulting change in high-latitude planetary albedo is notably different in the *q*-flux and fixed current experiments. In the latter case, strengthened ocean currents cause a substantial reduction in the amount of sea ice and, in the Northern Hemisphere, of snow over the land, thus decreasing the surface albedo (Fig. 4). However, the interaction between sea ice and cloud cover can reduce the impact of the surface albedo change on the TOA (this will be discussed in Section 3.1.2). Due to experimental design the true impact of sea ice and land snow on global mean temperature is not identified in the *q*-flux experiments. Consequently OHT has little influence on high-latitude planetary albedo in these models (Figs 3a and b). For the CCM3 model this arises as the sea ice cover is not allowed to change—which is obviously unrealistic. In the GISS model this is because, even though the extent of sea ice and Northern Hemisphere snow cover decrease, the surface albedo of regions covered with sea ice and land snow is often unrealistically low. The fixed current experiments may, however, exaggerate the albedo of sea ice since the GFDL model does not allow snow to age on ice (Winton, 2003). The model experiments most likely bracket the true effect of OHT on the sea ice albedo feedback.

3.1.2. The role of clouds. Figure 5 shows the change in the area-weighted, zonally averaged low, medium and high cloud cover along with the change in SWR reflected at the TOA when OHT is introduced or increased in the three models. The change in mid- and high-level cloud cover is largest at tropical latitudes where the area of warm water spreads with the introduction of OHT, decreasing deep convection over the cooler deep tropical waters (10°S–6°N), whilst increasing deep convection over the surrounding tropics. These cloud changes to a large extent

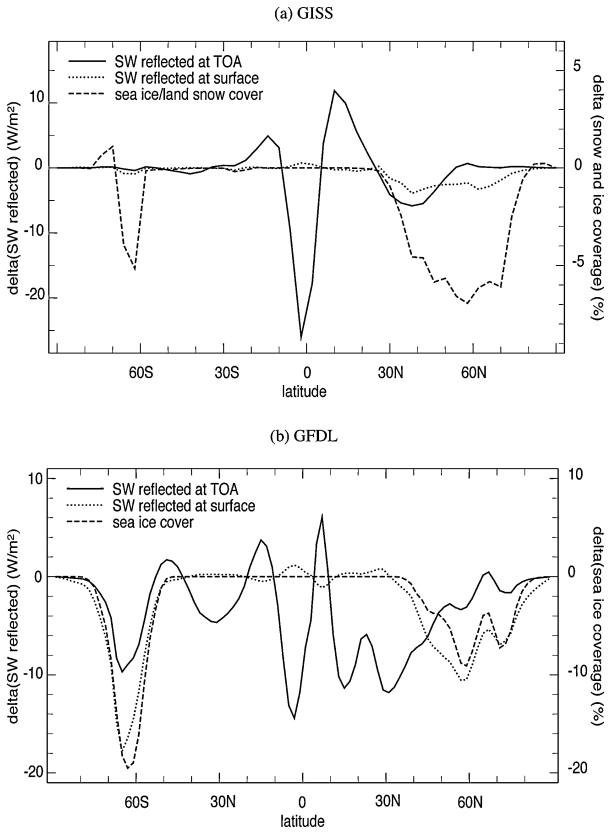

Fig. 4. The annual mean difference in the zonally averaged, area-weighted SWR reflected at the surface and at the TOA, along with the percentage change in sea ice/land snow due to OHT: (a) control—no flux, GISS AGCM OML, (b) 150%–50% fixed currents, GFDL AM2 AGCM dynamic ocean (sea ice change only—land snow data not saved). Not shown for CCM3 as sea ice was held fixed in this experiment.

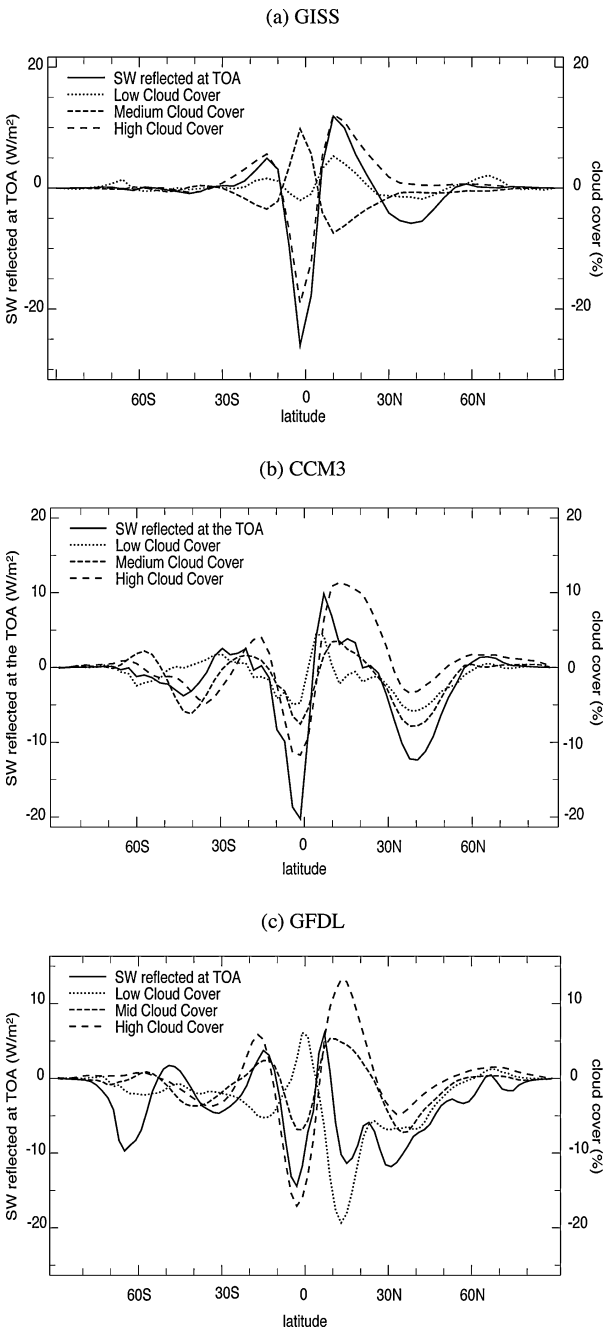

Fig. 5. The annual mean difference in the zonally averaged, area-weighted low, mid and high cloud amount (%), and the zonally averaged SWR reflected at the TOA due to OHT (in $W\,m^{-2}$): (a) control—no flux, GISS AGCM OML, (b) control—no flux, CCM3 AGCM OML, (c) 150%–50% fixed currents, GFDL AM2 AGCM dynamic ocean.

control the changes in total OLR, particularly at tropical latitudes where the changes in cloud cover are substantial (Fig. 6). However, changes in tropical deep convective clouds introduce opposite sign changes of equal magnitude in OLR and net SWR at the TOA. As such, the net radiative impact of these cloud changes when heat transport by the oceans increases is small in the models.

The role of low-level cloud changes is strikingly different between the GFDL fixed current model, on one hand, and the CCM3 and GISS models on the other hand. In the GFDL model, low clouds decrease everywhere from 4°N–60°N with strengthened ocean currents (Fig. 5c). The change in low cloudiness at subtropical latitudes (20°–40° latitude) is associated with a decrease in trade cumulus and marine stratus cloud cover (Winton, 2003). This change is most pronounced in the Northern Hemisphere and explains much of the decrease in planetary albedo at subtropical latitudes. Low clouds have a net cooling effect on climate as they have little impact on OLR, while increasing planetary albedo. Winton (2003) attributes the reduction in low clouds to the decreased lower atmospheric stability associated with the reduced meridional tropical SST gradient as OHT strengthens (Miller, 1997; Clement and Seager, 1999). This

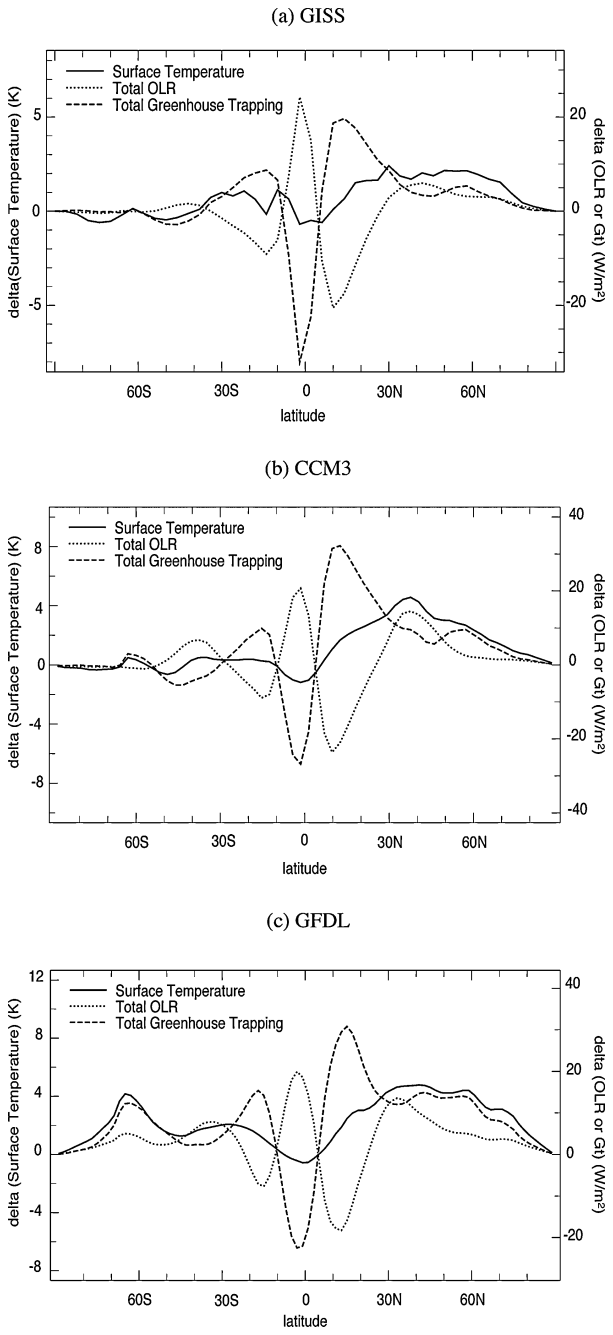

Fig. 6. The annual mean difference in the zonally averaged, area-weighted surface temperature (in K), total OLR and total greenhouse trapping (both in W m^{-2}) for (a) GISS AGCM OML control minus no OHT, (b) CCM3 AGCM OML control minus no OHT, (c) 150%–50% fixed currents, GFDL AM2 AGCM dynamic ocean.

relationship between stability in the lower atmosphere and low cloud cover was first empirically observed by Klein and Hartmann (1993). Mechanistically, decreased atmospheric stability affects the amount of low cloud by increasing the entrainment of drier air from above the boundary layer, reducing relative humidity and hence suppressing cloud formation.

Subtropical low clouds in the q-flux experiments are much less sensitive to the introduction of OHT. As such the subtropical reduction in planetary albedo is significantly smaller, particularly in the GISS model (Fig. 5). Although the q-flux and fixed current experiments both show decreased atmospheric stability with increasing OHT, the GFDL model used in the fixed current experiments better captures the relationship between low cloudiness and lower atmospheric stability (Winton, 2003). As such, the GFDL model's predicted changes in low cloudiness are probably more realistic than those in the GISS and CCM3 models.

As briefly explained in Section 3.1.1, the increase in OHT in the GFDL model causes a reduction in the amount of sea ice and, in the Northern Hemisphere, of land snow, thus reducing the planetary albedo. This is partially opposed in the Southern Hemisphere, and almost perfectly compensated for in the Northern Hemisphere, by increased cloud cover (Fig. 5). The increase in high-latitude total cloud cover may be due to increasing surface evaporation, as might be expected from surface warming over regions of sea ice retreat. Here, increased evaporation occurs in response to both the increase in ocean heat convergence and the increase in solar radiation absorbed by the oceans. The net radiative cooling effect of these clouds to some degree damps the increase in surface temperature driven by the decreased sea ice extent and surface albedo. The net result is that in the GFDL model OHT reduces the planetary albedo in the Southern Hemisphere extratropics but leaves it largely unchanged in the Northern Hemisphere extratropics (Fig. 3).

Within the deep tropics, the redistribution of clouds with increased OHT has a minor impact on the net TOA radiation: much of the change in greenhouse trapping associated with clouds is cancelled by an opposing change in SWR at the TOA (Fig. 7). Such a cancellation of long-wave and short-wave effects occurs as the largest change in cloudiness is seen for the deep convective clouds. Consequently, in this region much of the climate change is due to atmospheric water vapour in the clear-sky portions.

3.1.3. The role of water vapour. Figure 8 shows the zonal mean change of clear-sky OLR and clear-sky G_t, surface temperature, T_s and the change in column integrated atmospheric water vapour mass, M_q, due to introducing or strengthening OHT in the three coupled models. As expected, there is an inverse relationship between the change in OLR (both total and clear-sky) and atmospheric moisture. The inclusion of OHT causes a drying of the deep tropical atmosphere and a significant increase in the atmospheric water vapour content over the rest of the tropics and subtropics. This is associated with the meridional extension of the area of warm SSTs, and hence an increase in clear-sky greenhouse trapping. Consequently, over extensive regions of the tropics and subtropics, particularly between 3° N and 20° N, despite surface warming, the clear-sky OLR actually *decreases* due

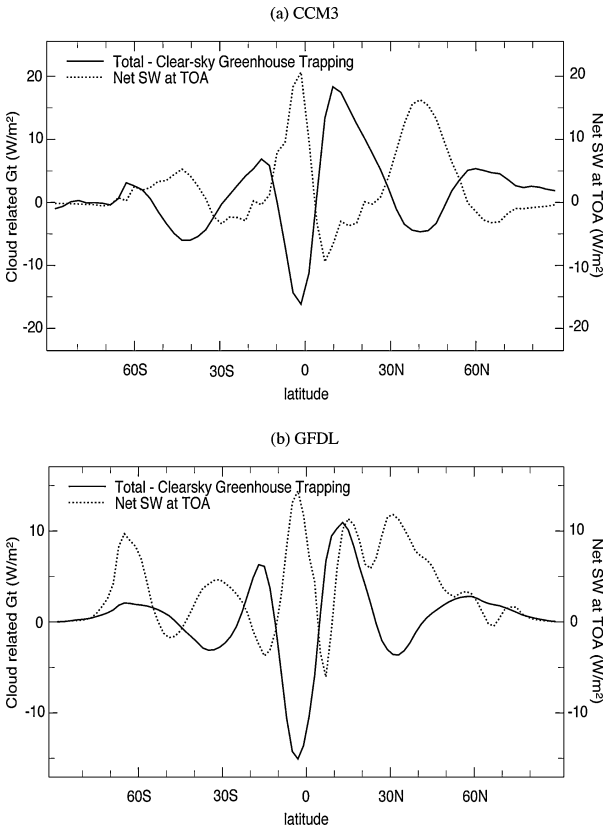

Fig. 7. The annual mean difference in the zonally averaged, area-weighted 'total minus clear-sky' greenhouse trapping and the zonally averaged SWR at the TOA due to OHT (both are in W m^{-2}): (a) control—no flux, CCM3 AGCM OML, (b) 150%–50% fixed currents, GFDL AM2 AGCM dynamic ocean.

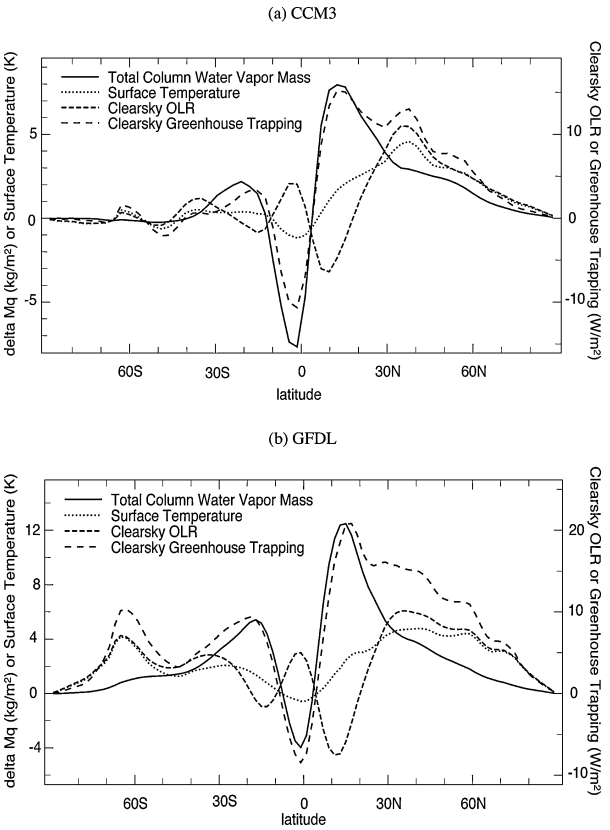

Fig. 8. The annual mean difference in the zonally averaged, area-weighted column integrated water vapour mass (M_q in kg m^{-2}), surface temperature (in K), clear-sky OLR and clear-sky greenhouse trapping (both in W m^{-2}) for (a) CCM3 AGCM OML control minus no OHT and (b) 150%–50% fixed currents, GFDL AM2 AGCM dynamic ocean. Clear-sky and cloudy-sky component data for the q-flux experiments using the GISS model were not saved.

to increased greenhouse trapping associated with the moistening of the atmosphere. Here the change in OLR is a positive feedback on surface temperature. At latitudes polewards of 20° where surface temperatures also increase due to OHT, the OLR increases and is a negative feedback on the temperature change.

In both the current climate, as well as the modelled climates with no or reduced OHT, the subtropical atmosphere has relatively little water vapour in comparison to the moist, convective system of the deep tropical atmosphere. As such, increasing the moisture content of the subtropics has a significantly larger feedback on the subtropical surface temperature, via the amount of greenhouse trapping, than reducing the deep tropical moisture content by the same amount (Fig. 8). This is because the atmospheric infrared (IR) opacity increases roughly logarithmically with water vapour concentration (Cess, 1974). Consequently, the meridional redistribution of atmospheric moisture, drying the moist deep tropics and moistening the dry subtropics and mid-latitudes, results in a smaller cooling in the near equatorial region than warming in the subtropics. This contributes to the global mean warming.

This redistribution of atmospheric moisture when the oceans transport more heat must also be explained. The cooling of the upper deep tropical troposphere is greater than the tropical surface cooling (Fig. 11). This is principally because of the increased moist adiabatic lapse rate of convective air parcels arising from a cooler surface. Consequently, the colder deep tropical troposphere holds less water vapour in the case where OHT is included/strengthened. Similarly, the warming of the subtropical troposphere coincides with moistening as the amount of water vapour the atmosphere can hold becomes greater. However, because the distribution of water vapour is greatly influenced by the atmospheric circulation, the regions of temperature change and moistening do not perfectly match.

Figure 9 shows the impact of including/strengthening OHT on the zonally averaged specific humidity and meridional stream function of the atmosphere. In the zonal mean the changes in the distribution of water vapour caused by including/strengthening OHT correspond closely to changes in the meridional stream function at tropical and subtropical latitudes, particularly in

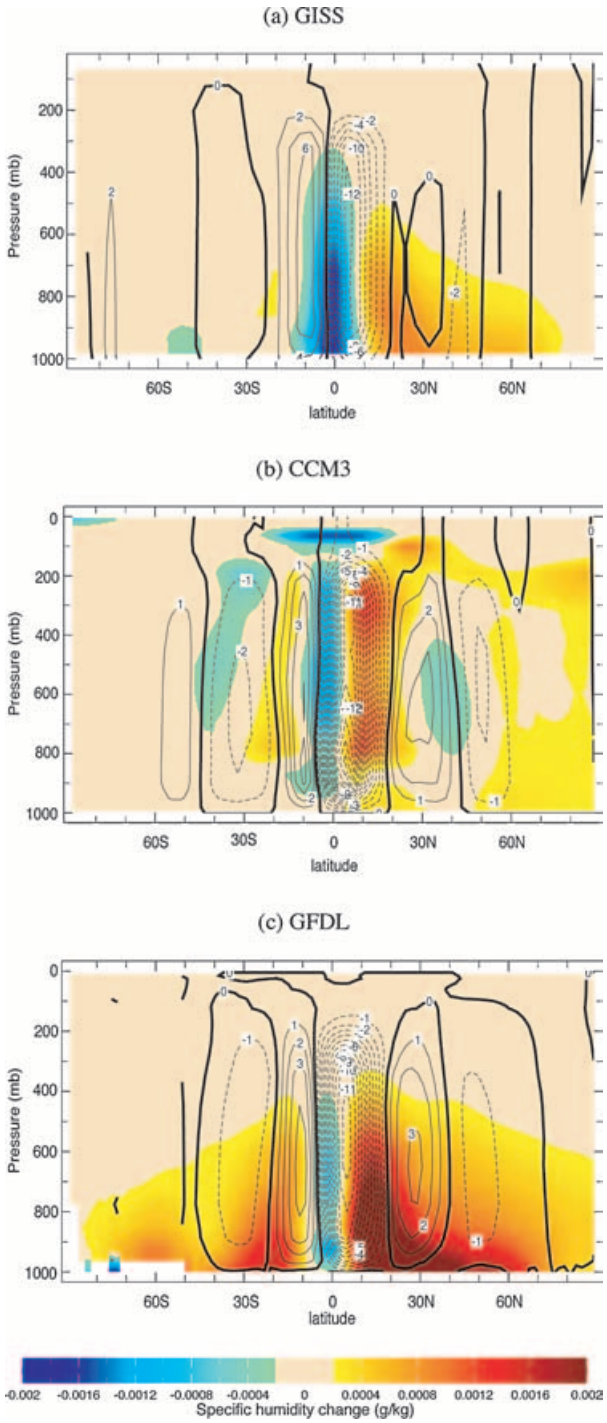

Fig. 9. The difference in the annual zonally averaged specific humidity (colours, g kg^{-1}) and atmospheric meridional stream function (contours, 10^{10} kg s^{-1}) for (a) control—no flux GISS AGCM OML, (b) control—no flux CCM3 AGCM OML and (c) 150%–50% fixed currents, GFDL AM2 AGCM dynamic ocean.

the CCM3 model. With more heat transport in the ocean, the Hadley cell weakens and the warm pool and associated region of widespread convection spreads further from the equator, giving rise to drier deep tropics and moister subtropics. It is for this reason that we will refer to the increased subtropical moisture as a positive 'dynamical' water vapour feedback. By this we mean that while OHT warms the subtropics, which is expected to lead to moistening by thermodynamics alone, there is an additional effect whereby the atmospheric circulation response also moistens these regions further such that OLR is actually reduced: a positive *dynamical* feedback. At mid to high latitudes where moisture transport occurs primarily via stationary and transient eddies, rather than the large-scale overturning cells, the clear relationship between changes in moisture and zonal mean circulation do not apply.

A complementary way of explaining the dynamical reason for why the introduction of OHT causes the atmosphere to hold more water vapour than the global mean involves the interplay between convection and precipitation. The increase in the area of zonal mean atmospheric ascent with OHT spreads the region of convective activity and moistens off-equatorial regions that are relatively undersaturated. Similarly, with no or diminished OHT, atmospheric ascent, and hence convective activity, strengthens substantially and becomes equatorially confined. In this case the atmosphere receives an increased moisture flux in an area already close to 100% relative humidity and convective precipitation increases greatly in the deep tropics. Essentially this mechanism moistens the global atmosphere as OHT allows for more places of intermediate relative humidity where the vapour can accumulate without getting close to saturation and raining out.

The dynamical water vapour feedback occurs in addition to the atmospheric moistening that arises as a thermodynamic response to the warming caused by the reduction in planetary albedo. The change in atmospheric relative humidity with increased OHT can help to identify where the moistening is more than purely thermodynamic in origin, since the latter is not expected to change the relative humidity distribution radically. In all three models, a substantial change in relative humidity occurs throughout the tropics when OHT is increased, with reduced relative humidity in the deep tropics and increased relative humidity in the subtropics (Fig. 10). It is contended that these changes in relative humidity distribution arise from the dynamical response of the atmosphere to OHT and could not be caused by the thermodynamic water vapour feedback.

In summary, all three coupled model climates readjust themselves to the incorporation of OHT by not only redistributing the atmospheric water vapour but also by moistening in the global mean (Table 1). This is a fundamental cause of the global mean warming that accompanies the introduction of OHT: the mean global surface temperature increases as OHT increases the greenhouse trapping of the global mean atmosphere. The increase in greenhouse trapping is caused by two mechanisms. The first concerns the dynamically driven redistribution of atmospheric

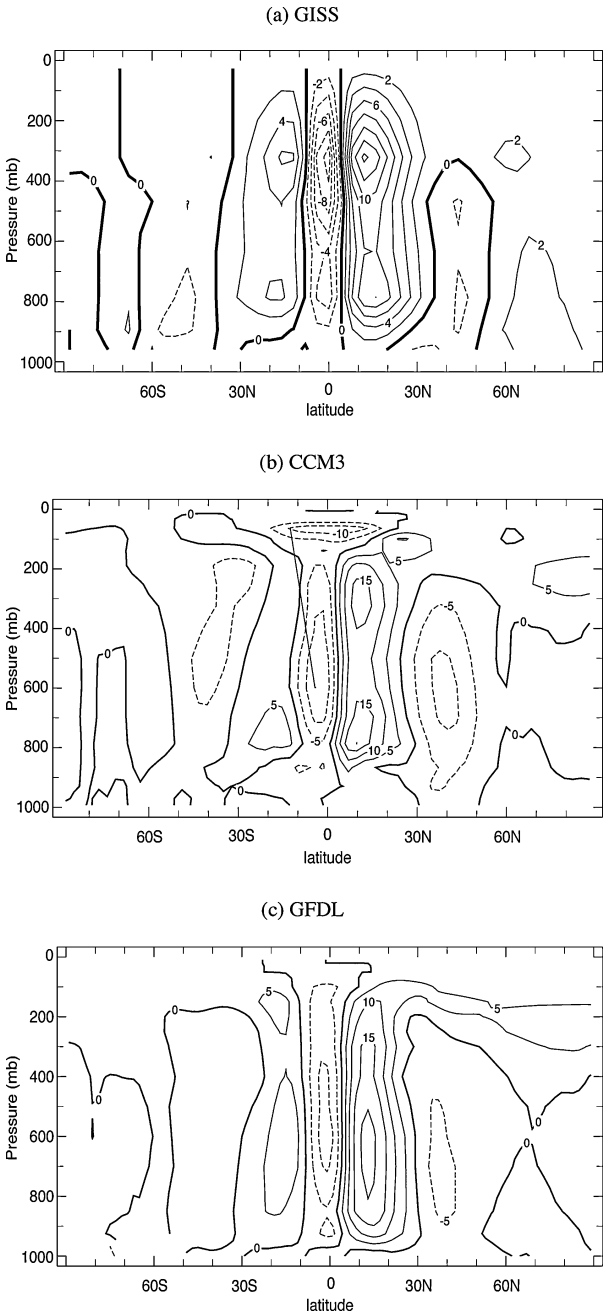

Fig. 10. Zonal mean relative humidity difference (%) for (a) control—no flux GISS AGCM OML, (b) control—no flux CCM3 AGCM OML and (c) 150%–50% fixed currents, GFDL AM2 AGCM dynamic ocean.

water vapour. The second is thermodynamic in origin and is a response to the warming caused by the reduction in planetary albedo caused by the decrease in sea ice/land snow and the decrease in subtropical cloud. Separating these two effects is difficult, but clearly they are both important for climate warming with increased OHT.

3.1.4. The role of atmospheric lapse rate changes. There is an additional feedback that must be addressed. Although the extratropical atmosphere, like that of the subtropics, moistens with increased heat transport by the oceans it is clear that here the change in clear-sky greenhouse trapping is too large to be explained by the change in column integrated atmospheric water vapour, M_q (Fig. 8). Clear-sky greenhouse trapping can increase even if the moisture content of the atmosphere remains fixed, simply due to a change in the atmospheric lapse rate.

If the surface warming exceeds the tropospheric warming at the local emission level (i.e. the atmospheric lapse rate increases), the surface long-wave emission will increase more than that at the emission level, and greater long-wave trapping will occur. In general this lapse rate feedback applies to all latitudes. However, at low latitudes both the relative abundance of atmospheric water vapour and the inability of the tropical troposphere to deviate from a moist adiabatic lapse rate reduce its impact relative to the water vapour feedback. In contrast, at northern midlatitudes, and at high latitudes of both hemispheres, the lapse rate increases with OHT present or strengthened (Fig. 11), in the direction that increases clear-sky greenhouse trapping (Fig. 8).

At high latitudes, where near-surface temperature inversions occur, this lapse rate feedback is particularly prevalent if OHT is allowed to interact with the sea ice. As an example, going from 45°S to 65°S in Fig. 8b, while the increase in atmospheric moisture due to strengthened currents is modest, the added surface warming of approximately 2.5 K is accompanied by a 6 W m^{-2} increase in clear-sky greenhouse trapping. Increased ocean heat convergence warms the surface polewards of 40°N and 50°S as a result of the retreat of sea ice and/or land snow and hence an increase in surface short-wave absorption (Fig. 4b). At these latitudes the presence of a temperature inversion acts to confine the thermal response to low levels, such that upper tropospheric temperatures remain relatively unchanged (Fig. 11b). The resulting steepened lapse rate leads to greater greenhouse trapping, enhancing the initial warming at the surface. In summary, the high-latitude increase in clear-sky greenhouse trapping is due to a temperature-dependent feedback arising from the sea ice retreat, while in the subtropics a positive 'dynamical' water vapour feedback is important.

3.2. Adjustments in the net radiation balance and heat transport

The changes in heat transport and net radiation must be consolidated. When OHT is included or increased the total HT out of the tropics (i.e. the sum of that across 30° N and 30° S) increases by approximately 1 PW (Fig. 1). This increase in heat export from the tropics must be balanced by a net radiative gain in the region. A 1 PW increase in the sum of poleward HTs across 30°N and 30°S requires a 4 W m^{-2} increase in net incoming radiation at the TOA. In all three models the increased heat export out of the tropics goes hand in hand with both a reduction in

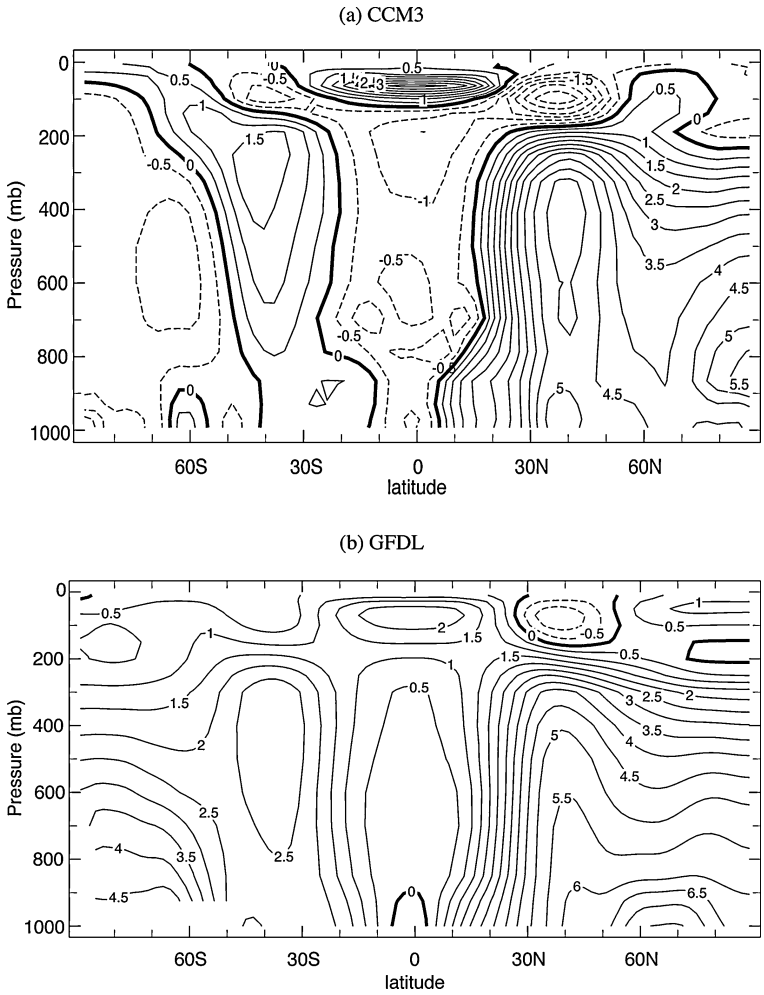

Fig. 11. Zonal mean atmospheric temperature difference (in K) for (a) control—no flux CCM3 AGCM OML (fixed sea ice) and (b) 150%–50% fixed currents, GFDL AM2 AGCM dynamic ocean (dynamic sea ice).

the OLR (Fig. 6) and in the SWR reflected at the TOA (Fig. 3) over the mean tropics. These changes amount to an increase of approximately 4 W m^{-2} in TOA incoming radiation, consistent with the increased total HT across the northern and southern boundaries. The OLR decrease occurs in spite of a warming of the tropical mean surface temperature with increased OHT. The changes in OLR and reflected SWR are brought about by the redistribution of atmospheric moisture and clouds as outlined in Section 3.1.

4. Discussion and conclusions

To examine the role of OHT on climate, two contrasting coupled GCM experiments were performed: the *q*-flux and fixed-current experiments. The first approach was carried out using two AGCMs—GISS model II and CCM3—coupled to mixed layers with and without OHT. The fixed-current approach coupled the GFDL AM2 model to a full-depth kinematic ocean in which currents were uniformly reduced and increased by 50% (Winton, 2003). In both, we examined how the climate responds to a situation in which the oceans carry more heat polewards. We focused upon how the climate adjusts to this change in OHT through a change in the distribution and effectiveness of its radiative absorbers and reflectors—clouds, water vapour, sea ice and land snow.

OHT warms the global mean climate in all three coupled models. The 1–1.6 K global mean warming in the *q*-flux experiments probably underestimates the global mean temperature response to OHT due to an unrealistic representation of the sea ice albedo feedback and an inability to capture the changes in subtropical low cloud cover that accompany the modelled changes in lower atmospheric stability. A more accurate representation of these climate feedbacks would potentially add a further warming, as both respond to increased OHT by decreasing the planetary albedo in the global mean. The larger 3.5 K global mean warming of the fixed current experiments, which use a model with better representation of low-level marine clouds, supports this result. However, in these experiments the high-latitude warming may be somewhat overestimated due to problems associated with the treatment of the albedo of perennial snow on ice.

Much of the global mean warming can be attributed to an increase in the greenhouse trapping of the global atmosphere (Table 1), primarily in the clear sky. This is caused both by the dynamically driven water vapour feedback that relates to changes in atmospheric circulation, and by the familiar thermodynamic water vapour feedback in response to the reduction in planetary albedo. The global atmospheric moisture content increases when OHT is introduced, with the most significant increase in greenhouse trapping occurring away from the equator but in the tropics and subtropics. As such, the signature of the increased water vapour feedback is most pronounced in the warming of these tropical/subtropical regions where the dynamical water vapour feedback plays a crucial role. An additional feedback associated with enhanced clear-sky greenhouse trapping at high latitudes involves a change in the atmospheric lapse rate. The remaining warming is due directly to the decrease in planetary albedo associated with reduced subtropical and mid-latitude low cloudiness, along with diminished sea ice cover at high latitudes.

One of the main conclusions of this work is the importance of understanding the influence of the water vapour feedback on climate not solely in terms of thermodynamics but also in the context of how the dynamical impact of varying ocean and atmospheric circulations affects the water vapour distribution. It has been shown that the redistribution of atmospheric water vapour by large-scale circulation changes has important implications for the mean climate of the tropics and the planet. In this study, incorporating OHT introduces a region where the OLR actually goes down despite surface warming—a positive 'dynamical' water vapour feedback. In this way OHT acts to warm the global mean climate by spreading the region of atmospheric deep convection, moistening the drier subtropical atmosphere, increasing the global mean atmospheric moisture content and subsequently enhancing atmospheric greenhouse trapping. All three GCMs agree on the fundamentals of how water vapour changes cause OHT to warm the mean climate.

Given the dependence of the mean temperature of the planet on the partitioning of the total HT between the atmosphere and ocean, it will be interesting to investigate how the partitioning changes in response to changes in orbital forcing, irradiance, surface boundary conditions and trace gas concentrations, and how this influences the mean climates. The results reported here suggest that in each case there are likely to be interactions between radiative feedbacks and large-scale circulation that influence the change in mean climate. Our understanding of how this partitioning is determined needs to be improved.

5. Acknowledgments

We wish to thank Adam Sobel and Andy Lacis for many useful discussions on this topic. Many thanks also to Mark Cane, David Rind and Bruno Tremblay for helpful reviews of the paper. CH, RS and AC were supported by NOAA grant UCS10-CU-02165401-SCF and NSF grants ATM-9986072MW and ATM-9986515.

References

Betts, A. K. and Ridgeway, W. 1999. Climatic equilibrium of the atmospheric convective boundary layer over a tropical ocean. *J. Atmos. Sci.* **46**, 2621–2641.

Bishop, J. K. B. and Rossow, W. B. 1991. Spatial and temporal variability of global surface solar irradiance. *J. Geophys. Res.* **96**, 16 839–16 858.

Bjerknes, J. 1964. Atlantic air-sea interaction. *Adv. Geophys.* **10**, 1–82.

Cess, R. D. 1974. Radiative transfer due to atmospheric water vapor: global considerations of Earth-energy balance. *J. Quant. Spectrosc. Radiat. Transfer* **14**(9), 861–871.

Clement, A. C. and Seager, R. 1999. Climate and the tropical oceans. *J. Climate* **12**, 3383–3401.

Cohen-Solal, E. and Le Treut, H. 1997. CMIP subproject. Energetics of coupled models: role of oceanic heat transport on climate and climate change. *Tellus* **49A**, 371–387.

Del Genio, A., Yao, M., Kovari, W. and Lo, K. 1996. A prognostic cloud water parametrization for global climate models. *J. Climate* **9**, 270–304.

The GFDL Global Atmospheric Model Development Team 2004. The new GFDL global atmosphere and land model AM2/LM2: evaluation with prescribed SST simulations. *J. Climate* **17**(24), 4641–4673, doi:10.1175/JCLI-3223.1.

Gregory, J. and Mitchell, J. 1997. The climate response to CO_2 of the Hadley Center coupled AOGCM with and without flux adjustment. *Geophys. Res. Lett.* **23**, 1943–1946.

Hansen, J., Russell, G., Rind, D., Stone, P., Lacis, A. and co-authors 1983. Efficient 3-dimensional global-models for climate studies—model I and model-II. *Mon. Weather Rev.* **111**(4), 609–662.

Hazeleger, W., Seager, R., Cane, M. A. and Naik, N. H. 2004. How can tropical Pacific ocean heat transport vary?. *J. Phys. Oceanogr.* **34**, 320–332.

Held, I. M. 2001. The partitioning of the poleward energy transport between the tropical ocean and atmosphere. *J. Atmos. Sci.* **58**, 943–948.

Kiehl, J. T., Hack, J. J., Bonan, G. B., Boville, B. A., Williamson, D. L. and co-author 1998. The National Center for Atmospheric Research Community Climate Model: CCM3. *J. Climate* **11**, 1131–1149.

Klein, S. and Hartmann, D. 1993. The seasonal cycle of low stratiform clouds. *J. Climate* **6**, 1587–1606.

Lewis, J. P., Weaver, A. J., Johnston, S. T. and Eby, M. 2003. Neoproterozoic "snowball Earth": dynamic sea ice over a quiescent ocean. *Paleoceanography* **18**(4), 1092.

Li, Z. and Leighton, H. G. 1993. Global climatologiesof the solar radiation budgets at the surface and in the atmosphere from 5 years of ERBE data. *J. Geophys. Res.* **98**, 4919–4930.

Manabe, S., Bryan, K. and Spelman, M. J. 1975. Global Ocean-Atmosphere Climate Model. 1. Atmospheric circulation. *J. Phys. Oceanogr.* **5**(1), 3–29.

McPhaden, M. J. and Zhang, D. X., 2002. Slowdown of the meridional overturning circulation in the upper Pacific Ocean. *Nature* **415**(6872), 603–608.

Miller, R. L., 1997. Tropical thermostats and low cloud cover. *J. Climate* **10**(3), 409–440.

Poulsen, C. J., Pierrehumbert, R. T. and Jacob, R. L. 2001. Impact of ocean dynamics on the simulation of the Neoproterozoic "snowball Earth". *Geophys. Res. Lett.* **28**(8), 1575–1578.

Rind, D. and Chandler, M. 1991. Increased ocean heat transports and warmer climate. *J. Geophys. Res.* **96**, 7437–7461.

Russell, G. L., Miller, R. J. and Tsang, L. C. 1985. Seasonal oceanic heat transports computed from an atmospheric model. *Dynam. Atmos. Oceans*, **9**(3), 253–271.

Seager, R. and Blumenthal, M. B. 1994. Modeling tropical Pacific sea surface temperature with satellite-derived solar radiative forcing. *J. Climate* **7**(12), 1943–1957.

Seager, R., Murtugudde, R., Clement, A. and Herweijer, C. 2003. Why is there an evaporation minimum at the equator?. *J. Climate* **16**(22), 3793–3802.

Stone, P. H. 1978. Constraints on dynamical transports of energy on a spherical planet. *Dynam. Atmos. Oceans* **2**(2), 123–139.

Trenberth, K. E. and Caron, J. M. 2001. Estimates of meridional atmosphere and ocean heat transports. *J. Climate* **14**(16), 3433–3443.

Winton, M. 2003. On the climatic impact of ocean circulation. *J. Climate* **16**(17), 2875–2889.